ChemComm

Yield-prediction models for efficient exfoliation of soft layered materials into nanosheets

Journal:	*ChemComm*
Manuscript ID	CC-COM-03-2021-001440.R1
Article Type:	Communication

COMMUNICATION

Yield-prediction models for efficient exfoliation of soft layered materials into nanosheets

Kyohei Noda,[a] Yasuhiko Igarashi,[b,c] Hiroaki Imai,[a] Yuya Oaki*[,a,c]

Received 00th January 20xx,
Accepted 00th January 20xx

DOI: 10.1039/x0xx00000x

Yield-prediction models were studied for efficient exfoliation of soft layered materials stacked via van der Waals interaction by an assistance of machine learning on small experimental data. High-yield exfoliation of graphite and layered organic polymer were achieved in the conditions guided by the models in a limited number of experiments.

Layered materials and their exfoliated two-dimensional (2D) nanosheets exhibit emergent properties originating from the characteristic structures.[1] Nanosheets are obtained by exfoliation of the precursor layered materials in liquid phase.[2] In the present work, nanosheets are defined as not only the monolayers but also thin layers with anisotropic structures exfoliated from the layered materials. A typical method for liquid-phase exfoliation is sonication to apply mechanical stress.[2] The new methods have been studied to promote the exfoliation more efficiently, such as addition of specific exfoliating agents and assistance of microwave.[2d,3] A couple of previous reports showed high-yield syntheses of graphene and transition-metal dichalcogenides.[3] However, nanosheets are not always obtained in high yield through exfoliation. In particular, the guideline to select the dispersion media is required for liquid-phase exfoliation. In recent years, layered materials have the types diversified from classical inorganic ones to new organic and hybrid ones, such as metal- and covalent-organic frameworks (MOFs and COFs) and 2D polymers.[4] If the high-yield conditions, such as exfoliation media, are efficiently predicted before the experiments, the design, synthesis, and exfoliation of new layered materials can be accelerated. Here we propose straightforward yield-prediction models for efficient exploration of organic solvents as the exfoliation media (Fig. 1).

[a] Department of Applied Chemistry, Faculty of Science and Technology, Keio University, 3-14-1 Hiyoshi, Kohoku-ku, Yokohama 223-8522, Japan.
[b] Faculty of Engineering, Information and Systems, University of Tsukuba, 1-1-1 Tennodai, Tsukuba 305-8573, Japan.
[c] JST, PRESTO, 4-1-8 Honcho, Kawaguchi, Saitama 332-0012, Japan
† Electronic Supplementary Information (ESI) available: [Experimental methods, Datasets, Aadditional microscopy images]. See DOI: 10.1039/x0xx00000x

Exfoliation methods and processes are different for different interlayer interaction of layered materials.[2d] The interlayer interaction is mainly classified into two types, electrostatic and van der Waals interactions. For example, layered materials based on van der Waals interaction, such as graphite, transition-metal dichalcogenides, and black phosphorus, are exfoliated into the nanosheets with dispersion in liquid phase.[1b–e,2b,c,4,5] On the other hand, layered compounds based on the electrostatic interaction, such as clays, layered double hydroxides, and transition-metal oxides, are delaminated with ionic exfoliating agents in aqueous and polar organic media.[1a,f,g,2a,d,6]

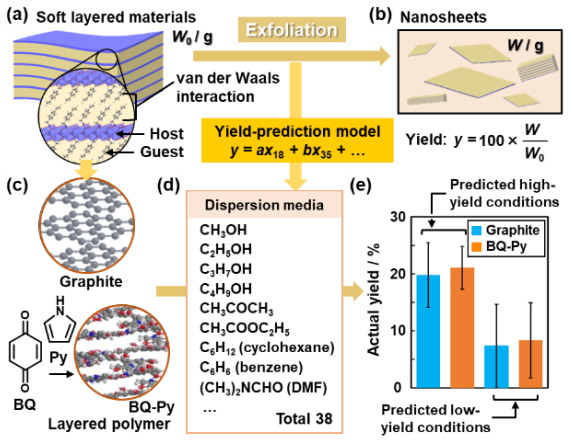

Fig. 1. Yield-prediction model for exfoliation of soft layered materials. (a) Structural model of soft layered composites based on the transition-metal oxide layers and interlayer organic guests. (b) Surface-modified nanosheets and definition of the yield in the present work. (c) Structural models of graphite and BQ-Py layered organic polymer for the predicted syntheses of the nanosheets. (d) Dispersion media for exploration of the high-yield conditions using the prediction model (Scheme S1 in the ESI). (e) Average actual yields for exfoliation of graphite (blue) and BQ-Py (orange) in the predicted high- (left bars) and low- (right bars) yield conditions.

Our group has studied a new exfoliation route using layered inorganic-organic composites.[1h,7] Transition-metal oxides stacking the layers via electrostatic interaction, a rigid type layered compound, are converted to the soft layered composites through intercalation of the organic guests (Fig. 1a).

As the weaker interlayer interaction via van der Waals interaction is introduced by the intercalated guests, the surface-modified nanosheets, including the monolayers and few-layers, are obtained through the exfoliation in organic dispersion media (Fig. 1b). The exfoliation behavior, such as yield and lateral size, is changed and controlled by the combinations of the host inorganic layers, guest organic molecules, and dispersion media.[7d–f] A yield-prediction model for exfoliation of the soft layered composites was constructed with an assistance of machine learning.[7d,e] The prediction model facilitates exploration of the guest-medium combinations achieving the high-yield exfoliation. As the main interlayer interaction of the soft layered composites is van der Waals interaction between the interlayer organic guests (Fig. 1a), the model can be applied to other layered compounds based on van der Waals interaction even without the interlayer guests, such as graphite and layered organic polymers (Fig. 1c). In the present work, the high-yield exfoliation of layered compounds stacked via van der Waals interaction was demonstrated using the yield-prediction model (Fig. 1c–e). Then, the prediction model was modified for the soft layered compounds. Moreover, the higher yield was achieved using the modified prediction model. The prediction models can be regarded as a general guideline for exploration of exfoliation media.

Table 1. Measured yields of the exfoliated nanosheets from graphite and BQ-Py in the predicted high- and low-yield conditions.

Predicted high-yield conditions (top)			Predicted low-yield conditions (bottom)		
Host	Graphite	Yield	Host	Graphite	Yield
Rank	Medium	y / %	Rank	Medium	y / %
1	1,3-Dioxolane	15.97	1	Hexane	1.74
2	Benzyl alcohol	24.88	2	Heptane	5.14
3	2-Methoxyethanol	14.94	3	Cyclohexane	9.62
4	2-Ethoxyethanol	14.80	4	Octadecene	20.39
5	2-Aminoethanol	28.29	5	Benzene	0
	Average	19.78		Average	7.38
	Standard deviation	5.68		Standard deviation	7.29
Host	BQ-Py	Yield	Host	BQ-Py	Yield
Rank	Medium	y / %	Rank	Medium	y / %
1	Benzyl alcohol	19.86	1	Hexane	0
2	Benzaldehyde	25.72	2	Heptane	3.28
3	Ethylene Glycol	14.55	3	Acetonitrile	17.31
4	Chlorobenzene	23.04	4	Cyclohexane	6.45
5	2-Methoxyethanol	22.04	5	4-methyl-2-pentanone	14.62
	Average	21.04		Average	8.33
	Standard deviation	3.75		Standard deviation	6.61

Graphite was selected as a model of crystalline layered compounds. An amorphous layered organic polymer was prepared by random 2D copolymerization of benzoquinone (BQ) and pyrrole (Py) with the simultaneous stacking (Fig. 1c and Fig. S1 in the Electronic Supplementary Information (ESI)), according to the method in our previous report.[8] These two soft layered materials were exfoliated into the nanosheets in organic dispersion media. The dispersion media achieving the high-yield exfoliation were explored in 38 common solvents using the yield-prediction model (Fig. 1d and Scheme S1 in the ESI). The predicted yield (y') is described by (Eq. 1) using two descriptors, namely Hansen-solubility (similarity) parameter (HSP) hydrogen-bonding term of the dispersion medium (x_{18}) and HSP distance between the host layer and dispersion medium (x_{35}).[7e]

$$y' = 35.00x_{18} - 32.33x_{35} + 34.07 \quad \text{… (Eq. 1)}$$

The descriptors x_{18} and x_{35} were converted to the normalized frequency distribution such that the mean is 0 and standard deviation is 1. These descriptors were extracted from total 35 explanatory variables (x_n: n = 1–35) potentially related to the exfoliation of the layered composites in our previous works (Table S1 in the ESI).[7e] Three HSP terms of the host graphite, namely dispersion (D), polarity (P), and hydrogen bonding (H) terms, were referred to the previous report for the calculation of the HSP distance to the solvents (x_{35}).[5b] D, P, and H terms of the BQ-Py polymer were calculated on the structure of the oligomer (Fig. S1 in the ESI). Table 1 summarizes the recommended dispersion media to achieve the highest and lowest yields corresponding to the top and bottom 5 in the ranking of the predicted values (Table S2 in the ESI), respectively. The exfoliation experiments were carried out on these 20 conditions.

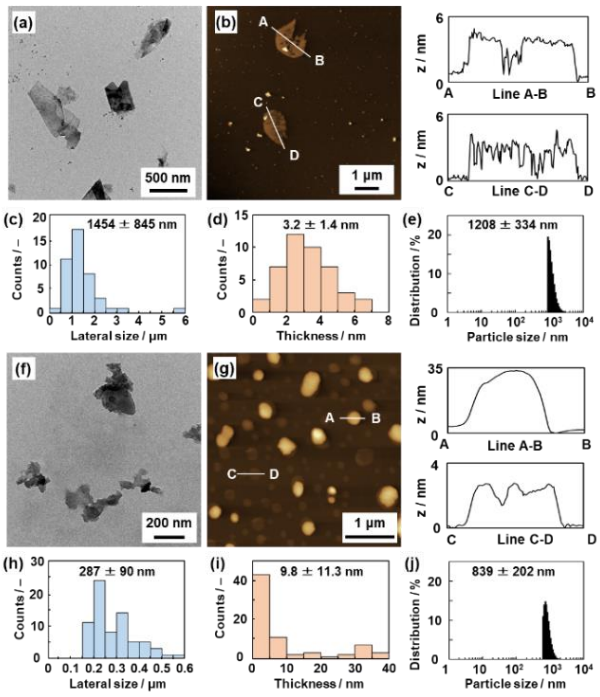

Fig. 2. Microscopy (a–d,f–i) and DLS (e,j) analyses of the nanosheets with exfoliation of graphite (a–e) in 1.3-dioxolane and BQ-Py (f–j) in chlorobenzene. (a,f) TEM images. (b,g) AFM images and their height profiles. (c,d,h,i) Histogram of the lateral size and thickness. (e,j) DLS charts of the dispersion liquids containing the nanosheets.

Graphite and BQ-Py were dispersed in these media. The dispersion liquids were sonicated at room temperature for 0.5 h in a sonic bath and then maintained at 60 °C for 0.5 h under stirring. The detailed method was described in the ESI. Then, the bulky unexfoliated and aggregated particles were removed by filtration. The dispersed nanosheets were suctioned and collected using a membrane filter with 0.1 μm in the pore size. The actual yield (y) was calculated using (Eq. 2) by the initial weight of the precursor layered materials (W_0) and weight of the collected nanosheets (W) (Fig. 1b).[7d–f]

$$y = 100 \times W / W_0 \quad \text{… (Eq. 2)}$$

The measured actual yields and their averages were summarized in Table 1. The average yields in the predicted high-

yield conditions (top five) were 19.78 ± 5.68 % for graphite and 21.04 ± 3.75 % for BQ-Py (*y* in the left part in Table 1 and Fig. 1e). On the other hand, the average yields in the predicted low-yield conditions (bottom five) were 7.38 ± 7.29 % for graphite and 8.33 ± 6.61 % for BQ-Py (*y* in the right part in Table 1 and Fig. 1e). The measured yields showed the significant differences in the predicted high- and low-yield conditions.

The exfoliated nanosheets were observed by transmission electron microscopy (TEM) and atomic force microscopy (AFM) (Fig. 3). The precursor layered materials had the average size 4.97 ± 4.10 μm for graphite and 2.26 ± 3.14 μm for BQ-Py (Fig. S2 in the ESI). The exfoliation of graphite in 1,3-dioxolane formed the nanosheets 1.45 ± 0.85 μm in lateral size and 3.2 ± 1.4 nm in thickness (Fig. 2a–d). Dynamic light scattering (DLS) analyses showed the particle-size distribution with the average size 1.21 ± 0.33 μm (Fig. 2e). Although the resultant nanosheets were not monolayered graphene, the anisotropic nanosheets stacking around 10 layers were obtained through the exfoliation. The BQ-Py nanosheets 287 ± 90 nm in lateral size and 9.8 ± 11.3 nm in thickness were obtained by the exfoliation in chlorobenzene (Fig. 2f–j). As the layers are partially cross-linked via covalent bond (Fig. S1 in the ESI),[8] the thicker nanosheets are formed for BQ-Py (Fig. 2g,i). These results support the formation of the nanosheets in organic dispersion media.

Table 2. List of the explanatory variables for ES-LiR.

n / –	Parameters	Unit	*n* / –	Parameters	Unit
	Dispersion media		16	[b]HSP dispersion	–
2	[b]Molecular length	nm	17	[b]HSP polarity	–
4	[a]Boiling point	°C	18	[b]HSP hydrogen bond	–
5	[a]Density	g cm^{-3}		Host-medium combination	
8	[a]Viscosity	cP	33	[b]Differences in dipole moment	Debye
10	[a]Surface tension	mJ m^{-2}			
14	[b]Dipole moment	Debye	35	[b]HSP distance	–

[a] Literature values. [b] Calculation values by commercial softwares (See ESI).

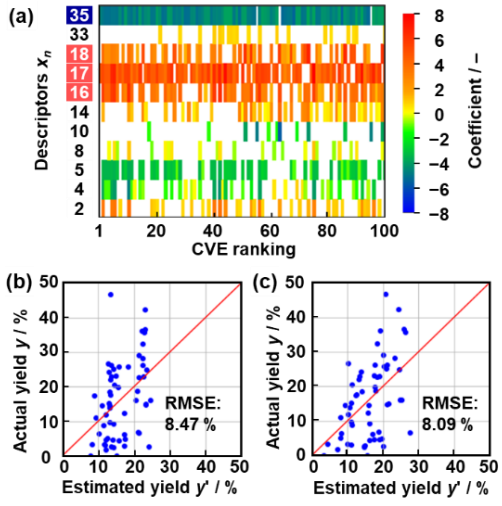

Fig. 3. Improvement of the prediction models. (a) Weight diagram of the ES-LiR analysis on total 60 data. (b,c) Relationship between the estimated (*y*′) and actual (*y*) yields for the prediction models using the two (x_{18} and x_{35}) (b) and four descriptors (x_{16} , x_{17}, x_{18}, and x_{35}) (c).

The high- and low-yield syntheses of the nanosheets were demonstrated in the predicted conditions using the model (Eq. 1). However, the model is constructed on the training data for the layered composites of host transition-metal oxide layers and interlayer organic guests (Fig. 1a).[7e] Here the descriptors and model are validated by machine learning (Fig. 3). New 40 yield data for exfoliation of graphite and BQ-Py were added to the original 20 data in Table 1 (Table S3 and Fig. S3 in the ESI). The actual yields (*y*) of the total 60 samples were set as the objective variables. We selected the potential descriptors (x_n: *n* = 2, 4, 5, 8, 10, 14, 16, 17, 18, 33, and 35 in Table 2) as the explanatory variables on the basis of our chemical perspective. The correlation between x_n and *y* was studied by exhaustive search with linear regression (ES-LiR),[9] a machine learning method for sparse modeling.[10] Sparse modeling is a recent data-scientific approach for description of high-dimensional data using a limited number of the strongly correlated factors, namely descriptors, on the assumption of the sparseness in the data. In ES-LiR, the linear multiple regression models are exhaustively constructed for all the possible combinations of the explanatory variables (x_i: *i* = 1, 2, 3, …*i*), namely total 2^N–1 (*N* = *i*) combinations. After the linear regression models are sorted in ascending order of the cross-validation error (CVE), the non-zero coefficient of the explanatory variables is represented by the warm and cool colors corresponding to the positive and negative values in the weight diagram (Fig. 3a). The more densely colored descriptors with the similar chromaticity are the potential descriptors. The weight diagram supports that x_{18} and x_{35} in (Eq. 1) are the descriptors with the positive and negative correlations, respectively (Fig. 3a). The yield-prediction model was modified to be (Eq. 3) using x_{18} and x_{35} with root mean squared error (RMSE) 8.47 % on the 60 training data for soft layered materials (Fig. 3b and Table S3 in the ESI).

$$y' = 4.37x_{18} - 5.88x_{35} + 16.21 \ldots \text{(Eq. 3)}$$

Fig. 3b shows the relationship between the estimated and actual yields. The more plots on the diagonal line mean the more accurate model with the correlation between the estimated and actual values. Moreover, the weight diagram indicates that x_{16} and x_{17} have potentials to be the descriptors with the positive correlation. The revised yield-prediction model was described using (Eq. 4) by x_{16}, x_{17}, x_{18}, and x_{35} with RMSE 8.09 % (Fig. 3c).

$$y' = 2.19x_{16} + 2.43x_{17} + 2.74x_{18} - 5.09x_{35} + 16.21 \ldots \text{(Eq. 4)}$$

The revised model using the four descriptors is more accurate because of the smaller RMSE value. The revised model (Eq. 4) has the improved correlation in the higher-yield conditions (Fig. 3b,c).

The correlation of these four descriptors is explained as follows. The higher yield is achieved by the smaller x_{35}. The smaller HSP distance between the layers and dispersion media means their higher affinity. The positive correlation of x_{16}, x_{17}, and x_{18} indicates that the higher yield is achieved in dispersion media with the larger HSP D, P, H terms. The stronger interactions of the dispersion media to the host layers contribute to achieve the higher yield. The other potential factors, such as the size and crystallinity, can be included as the explanatory variables in the training dataset. The prediction model can be improved and expanded with addition of the yield data by the similar manner.

The improved prediction model (Eq. 4) was applied to demonstrate the exfoliation of graphite in the higher yield using the mixed solvents as unknown dispersion media. As the coefficient of x_{35} is the largest in (Eq. 4), the dispersion media with the smaller HSP distance to graphite have potentials to achieve the high-yield exfoliation. HSP distance (HSP-d) is calculated by the differences in D, P, and H terms (δD, δP, δH) between two materials using (Eq. 5).[11]

$$\text{HSP-d} = \{4(\delta D)^2 + (\delta P)^2 + (\delta H)^2\}^{0.5} \quad \text{... (Eq. 5)}$$

Therefore, the dispersion media with D, P, and H terms similar to graphite provide the smaller HSP-d. According to the previous report,[23] the terms (D, P, H) of graphite are (18.0, 9.3, 7.3). The following pure solvents have the close values to graphite: (18.7, 3.6, 3.5) for chlorobenzene, (17.4, 13.7, 11.3) for DMF, (18.9, 8.0, 6.2) for benzaldehyde, (17.0, 11.0, 6.8) for acetylacetone, and (17.3, 9.2, 8.9) for 1,3-dioxolane. As the mixed solvents have the proportionally divided D, P, and H terms of the two pure solvents, the smaller HSP distances to graphite are achieved by the mixed solvents chlorobenzene-DMF, 1,3-dioxolane-benzaldehyde, and benzaldehyde-acetylacetone (Table S4 in the ESI). In addition, the D, P, and H terms themselves corresponding to x_{16}, x_{17}, and x_{18} in (Eq. 4) are large to achieve high-yield exfoliation, respectively. Exfoliation of graphite in the mixed solvents in 1/1 by volume actually showed the yield 48.01 % for chlorobenzene-DMF, 41.09 % for 1,3-dioxolane-benzaldehyde, and 14.41 % for benzaldehyde-acetylacetone for 1 h including the sonication at room temperature for 0.5 h and stirring at 60 °C for 0.5 h. The highest yield 48.01 % was not observed in the pure solvents as the dispersion media in the present work (Table S3 in the ESI). The yield is one of the highest efficiencies compared with previous works (Table S5 in the ESI).[4,7e] In this manner, the prediction model assists exploration of the dispersion media for the high-yield exfoliation in a limited number of the experiments. Efficient exfoliation of layered materials was reported using the mixed solvents and/or HSP values.[11b,12] However, the yield-prediction models as the guideline, such as (Eq. 3) and (Eq. 4), were not proposed in the previous works. The optimization of the exfoliation conditions has potentials for further improvement of the yield and selective syntheses of the monolayered graphene.

In summary, the yield-prediction models were studied for exfoliation of soft layered materials stacked via van der Waals interaction. The straightforward prediction model comprised few descriptors related to the physicochemical parameters of the host layers and dispersion media. The high-yield exfoliation of graphite and layered organic polymer was achieved in a limited number of the experiments, according to the prediction models. The straightforward model can be applied to design of new layered materials and exploration of the exfoliation media.

This work was supported by JST PRESTO (Y.O., JPMJPR16N2 and Y. I. JPMJPR17N2). There are no conflicts to declare.

Notes and references

1 (*a*) M. Osada and T. Sasaki, *Adv. Mater.*, 2012, **24**, 210; (*b*) V. Nicolosi, M. Chhowalla, M. G. Kanatzidis, M. S. Strano and J. N. Coleman, *Science*, 2013, **340**, 1226419; (*c*) M. Xu, T. Liang, M. Shi and H. Chen, *Chem. Rev.*, 2013, **113**, 3766; (*d*) H. P. Cong, J. F. Chen and S. H. Yu, *Chem. Soc. Rev.*, 2014, **43**, 7295; (*e*) J. R. Brent, N. Savjani and P. O'Brien, *Prog. Mater. Sci.*, 2017, **89**, 411; (*f*) P. Xiong, B. Sun, N. Sakai, R. Ma, T. Sasaki, S. Wang, J. Zhang, G. Wang, *Adv. Mater.* 2020, **32**, 1902654; (*g*) M. A. Timmerman, R. Xia, P. T. P. Le, Y. Wang and J. E. ten Elshof, *Chem. Eur. J.*, 2020, **26**, 9084; (*h*) Y. Oaki, *Chem. Commun.*, 2020, **56**, 13055.

2 (*a*) Q. Wang and D. O'Hare, *Chem. Rev.*, 2012, **112**, 4124; (*b*) A. Clesielski and P. Samori, *Chem. Soc. Rev.*, 2014, **43**, 381; (*c*) P. Tao, S. Yao, F. Liu, B. Wang, F. Huang and M. Wang, *J. Mater. Chem. A*, 2019, **7**, 23512; (*d*) Y. Oaki, *Chem. Lett.*, 2021, **50**, 305.

3 (*a*) M. Matsumoto, Y. Saito, C. Park, T. Fukushima and T. Aida, *Nat. Chem.*, 2015, **7**, 730; (*b*) J. Zheng, H. Zhang, S. Dong, Y. Liu, G. T. Nai, N. S. Shin, H. Y. Jeong, B. Liu and K. P. Loh, *Nat. Commun.*, 2014, **4**, 2995; (*c*) H. Lin, J. Wang, Q. Luo, H. Peng, C. Luo, R. Qi, R. Huang, J. Travas-Sejdic and C. G. Duan, *J. Alloys Compounds*, 2017, **699**, 222; (*d*) S. Zhao, S. Xie, Z. Zhao, J. Zhang, L. Li and Z. Xin, *ACS Sustainable Chem. Eng.*, 2018, **6**, 7652.

4 (*a*) M. Servalli and A. D. Schlüter, *Annu. Rev. Mater. Res.*, 2017, **47**, 361; (*b*) K. Ariga, S. Watanabe, T. Mori and J. Takeya, *NPG Asia Mater.*, 2018, **10**, 90; (*c*) C. N. R. Rao and K. Paramoda, *Bull. Chem. Soc. Jpn.*, 2019, **92**, 441; (*d*) T. Hartman and Z. Sofer, *ACS Nano*, 2019, **13**, 8566; (*e*) D. Rodríguez-San-Miguel, C. Montoro and F. Zamora, *Chem. Soc. Rev.*, 2020, **49**, 2291.

5 (*a*) Y. Hernandez, V. Nicolosi, M. Lotya, F. M. Blighe, Z. Sun, S. De, I. T. Mcgovern, B. Holland, M. Byrne, Y. K. Gun'ko, J. J. Bolamd, P. Niraj, G. Duesberg, S. Krishnamurthy, R. Goodhue, J. Hutchison, V. Scardaci, A. C. Ferrari and J. N. Coleman, *Nat. Nanotch.*, 2008, **3**, 563; (*b*) A. O'Neill, U. Khan, P. N. Nirmalraj, J. Boland and J. N. Coleman, *J. Phys. Chem. C*, 2011, **115**, 5422; (*c*) J. N. Coleman, *Acc. Chem. Res.*, 2013, **46**, 14.

6 (*a*) C. Chen, L. Tao, S. Du, W. Chen, Y. Wang, Y. Zou and S. Wang, *Adv. Funct. Mater.*, 2020, **30**, 1909832; (*b*) T. Sasaki, M. Watanabe, H. Hashizume, H. Yamada and H. Nakazawa, *J. Am. Chem. Soc.*, 1996, **118**, 8329; (*c*) R. Ma, Z. Liu, K. Takada, N. Iyi, Y. Bando and T. Sasaki, *J. Am. Chem. Soc.*, 2007, **129**, 5257.

7 (a) M. Honda, Y. Oaki and H. Imai, *Chem. Mater.*, 2014, **26**, 3579; (b) G. Nakada, H. Imai and Y. Oaki, *Chem. Commun.*, 2018, **54**, 244; (c) Y. Yamamoto, H. Imai and Y. Oaki, *Bull. Chem. Soc. Jpn.*, 2019, **92**, 779; (d) G. Nakada, Y. Igarashi, H. Imai and Y. Oaki, *Adv. Theory Simul.*, 2019, **2**, 1800180; (e) K. Noda, Y. Igarashi, H. Imai and Y. Oaki, *Adv. Theory Simul.*, 2020, **3**, 2000084; (f) R. Mizuguchi, Y. Igarashi, H. Imai and Y. Oaki, *Nanoscale*, 2021, **13**, 3853.

8 S. Yano, K. Sato, J. Suzuki, H. Imai and Y. Oaki, *Commun. Chem.*, 2019, **2**, 97.

9 Y. Igarashi, H. Takenaka, Y. Nakanishi-Ohno, M. Uemura, S. Ikeda and M. Okada, *J. Phys. Soc. Jpn.*, 2018, **87**, 044802.

10 (a) R. Tibshirani, M. Wainwright and T. Hastie, S*tatistical Learning with Sparsity: The Lasso and Generalizations*, Chapman and Hall/CRC, Philadelphia, PA 2015; (b) Y. Igarashi, K. Nagata, T. Kuwatani, T. Omori, Y. Nakanishi-Ohno and M. Okada, *J. Phys. Conf. Ser.*, 2016, **699**, 012001.

11 (*a*) C. M. Hansen, *J. Paint Technol.* **1967**, *39*, 1047; (*b*) J. Qin, X. Wang, Q. Jiang and M. Cao, *ChemPhysChem*, 2019, **20**, 1069.

12 (*a*) K. Zhou, N. Mao, H. Wang, Y. Peng and H. Zhang, *Angew. Chem. Int. Ed.*, 2011, **50**, 10839; (*b*) L. Dong, S. Lin, L. Yang, J. Zhang, C. Yang, D. Yang and H. Li, *Chem. Commun.*, 2014, **50**, 15936; (*c*) A. Sajedi-Moghaddam and E. Saievar-Iranizad, *Mater. Res. Exp.*, 2018, **5**, 015045; (*d*) J. Zhang, L. Xu, B. Zhou, Y. Zhu and X. Jiang, *J. Colloid Interface Sci.*, 2018, **513**, 279; (*e*) D. Nakamura and H. Nakano, *Chem. Mater.*, 2018, **30**, 5333.